

HIGH RESOLUTION MASS SPECTROMETRY ANALYSIS OF RIBOSOMAL PROTEINS IN EXPERIMENTAL DIABETES

E. UYY, V.I. SUICA, R.M. BOTEANU, L. IVAN, F. SAFCIUC, F. ANTOHE

“Nicolae Simionescu” Institute of Cellular Biology and Pathology, 8 B.P. Hasdeu Street, district 5,
Bucharest, Romania

Corresponding author: felicia.antohe@icbp.ro

Received November 9, 2015

Abstract. The present study aimed to determine whether ribosomal proteins could be involved in the onset of diabetic state in the pulmonary tissue. Biochemical assays, electron microscopy and LC-MS/MS analysis were performed on detergent resistant membrane (DRM) microdomains isolated from the lungs of diabetic and non-diabetic mice models. Electron microscopy results showed a well-developed synthesis apparatus in diabetes, demonstrating a high metabolic activity. LC-MS/MS analysis revealed that hyperglycemia has a modulatory effect on the expression of eight ribosomal proteins that co-fractionated with DRMs, pointing out toward a possible novel regulatory pathway in the mechanism of microangiopathy installation in the diabetic lung.

Key words: mass spectrometry, type I diabetes, ribosomal proteins.

1. INTRODUCTION

Diabetes mellitus is associated with metabolic, hormonal, microvascular abnormalities and disturbances of the cardiovascular and the respiratory systems. The pathogenesis of the major long-term complications of diabetes mellitus is currently thought to involve a microangiopathic process, targeting kidneys, eyes and lung tissues [1]. The pulmonary microangiopathy shows the thickening of the alveolar capillary and pulmonary arteriolar walls and decreased lung capillary blood volume in patients with type I diabetes. Well documented, ultrastructural changes of the lung parenchyma and microvasculature in diabetics were reported in the last decades [2–4]. In addition, factors responsible for the development of abnormal lung mechanics in diabetes mellitus are the biochemical alterations of the lung connective tissue as changes in either collagen or elastin components [5–7]. These modifications can cause impaired lung function, decreased respiratory muscle endurance, diaphragmatic paralysis, dyspnea, pulmonary hypertension and pulmonary infections [8]. Recently published data underlines the essential roles of ribosomal proteins, not only in peptide biogenesis and protein translation, but also

as active macromolecules acting as regulatory proteins to execute numerous extra-ribosomal functions: p53 translation [9], cell signaling [10], NFkB interaction [11], antiviral co-factor [12], etc. Ribosomal proteins have been linked to several pathological conditions, including autoimmune diseases and human malignancies (breast, skin, colon, lung, ovarian tumors). In the last few years it was demonstrated that ribosomal proteins may be targeted to lipid rafts *via* S-acylation, possibly to facilitate regulation of ribosomal protein activity and/or dynamic synthesis of lipid raft proteins [13–14].

The present study, using high resolution liquid chromatography coupled with tandem mass spectrometry (LC-MS/MS), showed that hyperglycaemia modulates the protein expression of eight ribosomal proteins (Rplp0, Rplp2; Rpl19; Rpl15; Rps16; Rpl7; Rps3 and Rps11) that co-fractionated within detergent resistant membrane (DRM) microdomains. The co-localization of these ribosomal proteins with other resident signaling macromolecules in the DRMs demonstrates to have relevant significance in the regulation of pathological processes in diabetes.

2. MATERIALS AND METHODS

2.1. MATERIALS

All chemicals were of LC or MS grade, unless otherwise specified. Protease inhibitor cocktail *Complete* tablets were purchased from Roche (Mannheim, Germany). C18 solid phase extraction columns were acquired from Waters Corporation (Milford, MA, USA). Antibodies and their sources were as follows: Rabbit polyclonal Anti-ERK1 + ERK2 antibody ab17942; mouse monoclonal Anti-Erk1 (pT202/pY204) + Erk2 (pT185/pY187) ab50011 antibody clone MAPK-YT; mouse monoclonal anti-beta Actin ab6276 antibody clone [AC-15] from Abcam (Cambridge, UK) and anti-mouse or anti-rabbit IgG peroxidase conjugates from Sigma (St. Louis, MO., USA). The enhanced chemiluminescence Western blotting detection reagent kit was supplied by Thermo Scientific (IL, USA). All other reagents were purchased from BIO-RAD or Sigma.

2.2. EXPERIMENTAL DESIGN

Mice with genetically induced type I diabetes mellitus [15] were divided in two groups of six animals each: (1) double transgenic mice (dTg), Ins-HA^{+/-} TCR-HA^{+/-} that were demonstrated to rapidly develop an aggressive diabetes and (2) the corresponding control, single transgenic mice (sTg) Ins-HA^{+/-} TCR-HA^{-/-}. During the experiments, animals had free access to standard diet and fresh water. After 12 weeks, the animals were evaluated for changes of body weight and sera glucose

concentration; when hyperglycaemia reached pathological levels (435 ± 108 mg/dl), the animals were sacrificed and the lungs were harvested and processed for afterwards experiments. All animal studies were conducted in accordance with “International Guiding Principles for Biomedical Research Involving Animals” (Council for the International Organizations of Medical Sciences, December 2012), regulations of the ethic Committee of ICBP “N. Simionescu,” and Romanian Law no. 471/2002.

2.3. ELECTRON MICROSCOPY

The blood from anesthetized mice was washed out by perfusion with phosphate buffered saline followed by *in situ* fixation. Small lung fragments were processed for electron microscopy [16]. Thin sections (70 nm) were examined on a Philips 201C-electron transmission microscope.

2.4. DETERGENT RESISTANT MEMBRANE MICRODOMAINS ISOLATION

Detergent resistant membrane (DRM) microdomains were prepared as previously described [4]. Briefly, 200 mg of lung tissue fragments were solubilized on ice in 1.8 ml MES-buffered saline (MBS), pH 6.5 (containing: 25mM MES, 0.15M NaCl) and 1% Triton X-100 with the use of a rotor-stator mechanical homogenizer. The resulting lysate was fractionated by sucrose gradient centrifugation at $200\,000\times g$, for 18 hours at $4^{\circ}C$, using the Optima LE-80 ultracentrifuge (Beckman-Coulter, Fullerton, USA). Fractions ($n = 12$) were harvested from top to bottom, for biochemical determinations and afterwards experiments. The three fractions (4, 5 and 6) enriched in protein and cholesterol, were combined from each animal separately and diluted 5 times in MBS before a 4 hour ultracentrifugation ($200\,000\times g$, $4^{\circ}C$). The resulting supernatant was discarded and the pellet was processed for Western blot and mass spectrometry analysis.

2.5. IMMUNOBLOT PROTEIN ANALYSIS

20 μg of proteins were denatured in loading buffer and separated on a 12.5% SDS-polyacrylamide gels. For Western immunoblot analysis, separated proteins were electro-transferred onto a nitrocellulose membrane and incubated with primary anti-b-actin, anti-ERK1/2 or anti-Erk1 (pT202/pY204) + Erk2 (pT185/pY187) antibodies and secondary horseradish peroxidase-labeled anti-immunoglobulin antisera as described previously [17]. The reaction was quantified by densitometry with Scion Image freeware.

2.6. PREPARATION OF DRMs FOR MASS SPECTROMETRIC ANALYSIS

The samples were solubilized in buffer containing 8M urea, 1% sodium deoxycholate (DOC) and 0.1% Tris-HCl (pH 8.8) by powerful agitation for 30 min on ice, followed by occasional vortexing for another 3 hours on ice. The samples were then purified by precipitation with methanol/chloroform/water (4:2:4) mixture. The probes were further processed as previously described [18]. Proteolysis was performed overnight, at 37°C, using a 1:20 enzyme to substrate quantity ratio. Formic acid was added to the resulted peptide mixtures up to pH 2–3 for trypsin inhibition and DOC precipitation. The peptides were purified using SPE and concentrated using the *Concentrator plus* system (Eppendorf, Hamburg, Germany).

LC-MS/MS experiments were performed using the EASY-nLC II coupled to the LTQ-Velos Orbitrap MS. The pre-column (EASY column, 2 cm × 100 μm i.d., C18, 5 μm, 120 Å, Thermo Scientific) was connected to the analytical column (EASY column, 10 cm × 75 μm i.d., C18, 3 μm, 120 Å). A gradient of 3–25% acetonitrile with 0.1 % (v/v) formic acid over water with 0.1 % (v/v) formic acid at a flow rate of 300 nL/min was used. The MS was operated in a top 12 data-dependent configuration at 60 k resolving power for a full scan across the 350–1700 m/z domain and collision induced dissociation fragmentation mode for MS2. Protein identification was performed using Proteome Discoverer 1.4 (Thermo Scientific) and Mascot 2.4.1 (Matrix Science, London, UK) within the Homo sapiens organism in UniProtKB/SwissProt fasta database, build 04.2013. A maximum of 2 missed cleavage sites was allowed. False Discovery Rate (FDR) target was set below 0.05. SIEVE 2.1 software (Thermo Scientific) was operated for label free relative quantification and quality assessment, through Principal Component Analysis (PCA). The principal components were generated using dTg/sTg ratios of peptides abundance, unique to each protein, to calculate the relative abundance of their respective proteins. The following filters were applied: dTg/sTg >1.5 or and dTg/sTg < 0.67 and $p < 0.05$, over six biological replicates, each in three technical replicates. The projection of the quantitative data onto KEGG signaling pathways was performed within Protein Center software for determining their over-representation (FDR P-value < 0.05).

2.7. STATISTICS

All results were run in triplicate and expressed as mean ± SD. Raw data were analyzed by a student's unpaired t-test using Graphpad Prism 5.0 statistical software (GraphPad Software, La Jolla, CA). Significance was defined as $p < 0.05$.

3. RESULTS AND DISCUSSIONS

3.1. EXPERIMENTAL INDUCED DIABETES IN SMALL ANIMALS

All animals were sacrificed after 12 weeks. The dTg group showed a pathological increased serum glucose level (by 3 fold) and weight loss (by 1.2 fold) compared to control animal (sTg) – Fig. 1.

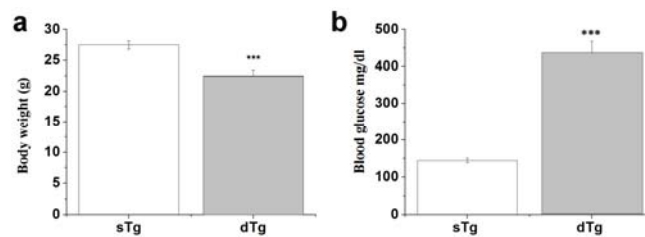


Fig. 1 – a) The diabetic mice (dTg) show significant weight loss (~1.2 times) after 12 weeks when compared with nondiabetic mice (sTg); b) blood glucose level of dTg group was ~3 times higher than the control sTg group, demonstrating the diabetic status of the animals.

Data are expressed as means \pm SD. *** $P < 0.001$ by Students t-test.

3.2. THE DIABETIC LUNG TISSUE PRESENTS A MODIFIED MORPHOLOGY

Electron microscopy of lung tissue sections from dTg mice revealed ultrastructure modifications in the diabetic animals. Specifically, the diabetic endothelium displayed a large number of membrane bound vesicles. All types of pulmonary cells presented a well-developed endoplasmic reticulum, numerous ribosomes and the extracellular matrix was considerably thicker than in sTg controls (Fig. 2a). These modifications were common characteristics of incipient pulmonary microangiopathy, while the ultrastructure of lung endothelium in controls (sTg) had the aspect of healthy vascular endothelium (Fig. 2b).

The ultrastructural modifications evidenced that type I diabetes mellitus induced noticeable alterations in lung parenchyma as response to hyperglycemia stress, paving the way towards diabetic-associated pulmonary dysfunction, in correlation with previous studies [2–4].

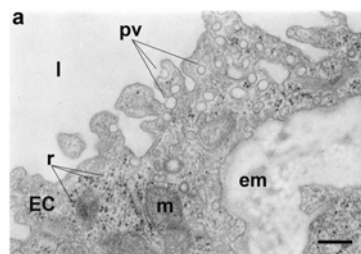
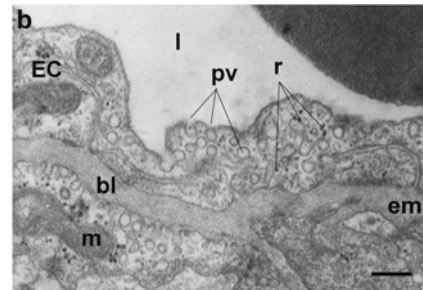


Fig. 2

Fig. 2 (continued) – Ultrastructure changes of lung capillary endothelial cells in double transgenic diabetic mice (a) compared with single transgenic mice (b). Note the presence of a highly convoluted apical plasmalemma, the noticeably increased number of plasmalemmal vesicles (pv) and ribosomes (r) and the hyperplastic extracellular matrix (em) in the double transgenic mice. l: capillary lumen; EC: endothelial cell; bl: basal lamina; m: mitochondria. Bars = 200 nm.



3.3. BIOCHEMICAL AND MASS SPECTROMETRIC CHARACTERIZATION OF DRMs

The Triton X-100-insoluble DRM complexes were recovered in fractions 4–6 (Fig. 3a), which were pooled together for each animal separately and further prepared for MS analysis.

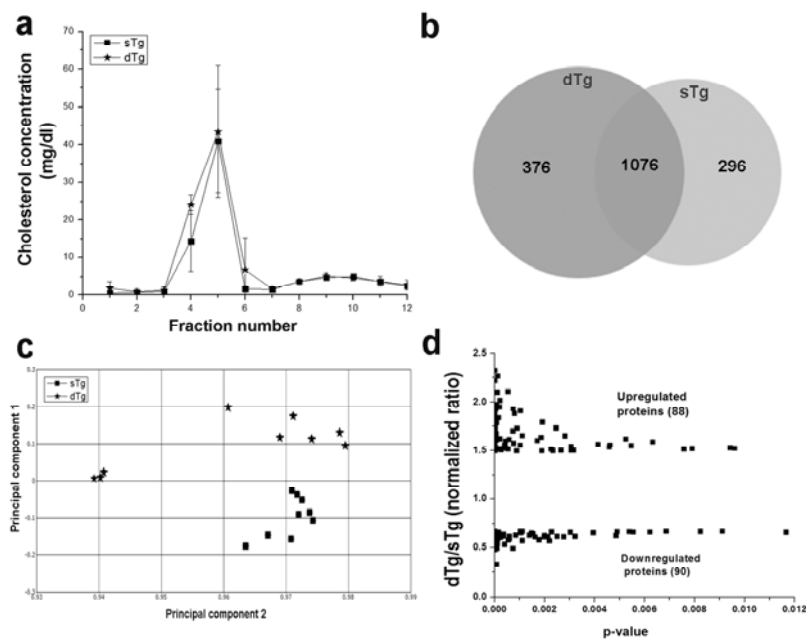


Fig. 3 – Characterization of isolated DRMs. (a) Cholesterol concentrations in fractions (1–12) obtained after ultracentrifugation of lung homogenate (3 independent experiments). (b) Venn diagram of the MS identified proteins in DRMs (fractions 4–6) representing merged experiments from all the technical and biological replicates of the diabetic (dTg) *versus* control tissue (sTg). Three sets of experiments were performed, each in technical triplicates. (c) Principal Component Analysis of filtered peptides isolated from dTg *versus* their sTg mice showing the biological significant differences between the two groups. (d) The up- and down-regulated ribosomal proteins normalized to the total ion current per MS experiment shown as dTg/sTg ratio, illustrated after the frame filtering (dTg/sTg > 1.5 or dTg/sTg < 0.67 and *p* value < 0.05).

LC-MS/MS experiments performed on DRMs isolated from dTg and sTg lung tissue led to the identification of a large number of proteins (1748 proteins). The unambiguously identified proteins from six biological replicates of dTg and sTg, respectively, were merged and retained for further analyses. 376 proteins were uniquely identified in dTg, 296 were found only in sTg, while 1076 were common to both groups (Fig. 3b). The relative quantification of the proteins evidenced a total of 88 proteins showing up-regulated abundance (1.5 fold increase of dTg/sTg ratio) while 90 proteins presented down-regulated expressions (0.67 fold lower of dTg/sTg ratio), (Fig. 3d). The post-filtering PCA revealed the excellent differentiation of the dTg and sTg groups. LC-MS/MS proteomic analysis evidently demonstrated that the replicates of the same biological condition clustered together on the same part of the PCA representation (Fig. 3c). At the same time, the two experimental conditions (sTg and dTg) revealed a distant partitioning from one another. The results indicated a consistent, underlying biological significance of diabetic *versus* non diabetic status. The list of differentially abundant proteins was correlated with KEGG databases and the *Ribosome* signaling pathway was found to be systematically overrepresented (FDR p -value = 2.66E-4). Within this pathway, the abundance of eight ribosomal proteins was found to be altered in dTg animals (Fig. 4a). These proteins were: 60S acidic ribosomal proteins P0 (Rplp0), P2 (Rplp2); 60S ribosomal proteins L15 (Rpl15), L19 (Rpl19), L7 (Rpl7); 40S ribosomal protein S16 (Rps16), S3 (Rps3) and S11 (Rps11).

The study demonstrated that hyperglycemia can modulate the abundance of eight ribosomal proteins that presumably bound to cellular membrane because they were co-fractionated in the DRMs. The results evidenced the upregulation of four ribosomal proteins (Rplp0, Rplp2, Rpl15, and Rpl19) in the diabetic compared with that of non-diabetic mice and the downregulation of the other four (Rps16, Rpl7, Rps3, Rps11) in the dTg *versus* sTg animals (Fig. 4a).

Lack of nutrients, including glucose starvation [14] was reported to disturb the process of ribosome biogenesis leading to accumulation of ribosome-free ribosomal proteins and thus leading to the ribosomal stress [19]. Ribosomal proteins have been linked to several conditions, including autoimmune diseases and human malignancies, which involve chronic inflammation. Over-expressed Rplp0, Rplp2, Rpl 19, Rpl 15 proteins are also reported in breast, colorectal, lung, gastric and/or prostate cancer [10, 20–25]. A study reported the presence of anti-Rplp0 and anti-Rplp2 in cerebrospinal fluid isolated from patients with neuropsychiatric systemic lupus erythematosus [24], showing the active implication of these proteins in inflammatory processes.

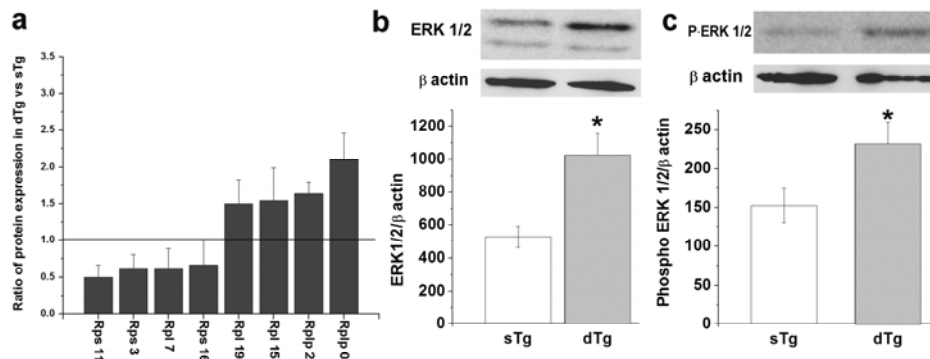


Fig. 4 – Expression of quantified ribosomal proteins shown as normalized ratio of dTg/sTg (a). Non-DRMs fractions (9–12) were analyzed by immunoblotting using anti-ERK1/2 (b), and anti-phospho-ERK1/2 (c) antibodies followed by the appropriate HRP coupled secondary antibodies. The levels of ERK1/2 and phospho-ERK1/2 were significantly increased in diabetes. β -actin served as loading control. Histograms show the means \pm SD. * $P < 0.05$.

Previous data demonstrated that Rplp0, dominantly expressed on the mammary vasculature during lactation, could be involved in receptor mediated endocytosis in endothelial cell culture model [27]. Rps3 has also an important role in oncogenesis [28] and in immune signaling [29–30]. Given the fact that Rps3 also activates the p53 tumor suppressive pathway, this ribosomal protein is regarded as one of the most fascinating ribosomal proteins with pivotal multifunctions [31]. Another study demonstrated that Rps16 gene is modified by progression of androgen-independent growth in human prostate cancer cells [32] and Rpl 7 was predicted as candidate biomarker in peripheral blood for monitoring cardiac allograft rejection [33].

Glucose can activate the mitogen-activated kinases, Erk-1/2, contributing to an increase in mitogenesis and protein synthesis, through an unknown phosphorylation mechanism. Our results demonstrated that the ERK1/2 level in group dTg was significantly increased (by 2-fold) comparable with the basal level of ERK1/2 in the control group (sTg) and a significant increase (by 1.6-fold) of phospho-ERK1/2 (T185+Y187) was observed in the lung tissue from the dTg group. This data supports the hypothesis that the hyperglycemic stress could be a causal factor for increased protein expression and phosphorylation of ERK1/2 at T185+Y187 (Fig. 4b–c), besides the specific modulation of the regulatory ribosomal proteins expression detected to be co-fractionated with DRM micro domains. We observed that the overexpression of Rplp0, Rplp2, Rpl 19 and Rpl 15 is very well correlated with increased ERK activity. Interestingly, Rpl 19 has been shown to stimulate the ERK activation [34] and may be involved in pathogenesis of autoimmune diseases and chronic inflammatory diseases.

4. CONCLUSIONS

In summary, we have demonstrated that pulmonary microangiopathy induced by type I diabetes mellitus was accompanied by modulatory effects on the abundance of eight ribosomal proteins that co-fractionated with detergent membrane microdomains. In addition, it is important to note that this study is the first that highlights an alteration of ribosomal protein expression in cellular membrane isolated from lungs affected by diabetes. This may represent an important direction to be pursued in elucidating the mechanism of lung diabetic microangiopathy installation.

Acknowledgments. We thank Radu Dorel Lucian, M.D., Ph.D., Associate Professor from “Cantacuzino” National Institute of Research and Development for Microbiology and Immunology, Bucharest, Romania for the transgenic-induced diabetes mice, Madalina Oppermann, Ph.D, for valuable collaboration, Mrs. Mariana Pascu for excellent technical assistance and Mrs. Misici Marilena for tissue sectioning. The present work was supported by the Romanian Academy and Ministry of Education and Research grant CNDI-UEFISCDI [PN-II-PCCA-2011-3 nos.: 153/2012] and CARDIOPRO project ID: 143, ERDF co-financed investment in RTDI for Competitiveness. E.U. and R.M.B acknowledge the support of the strategic grant POSDRU/159/1.5/S/133391-financed by the European Social Found within the Sectorial Operational Program Human Resources Development 2007–2013.

REFERENCES

1. U. Sankarasubbu, B. Kabali, World Journal of Medical Sciences **8**, 147-149 (2013)
2. D. Popov, M. Simionescu, The European Respiratory Journal (Eur Respir J) **10**, 1850-1858 (1997).
3. D. Popov, M. Simionescu, Italian Journal of Anatomy and Embryology **106**, 405-412 (2001).
4. E. Uyy, F. Antohe, L. Ivan, R. Haraba, D. L. Radu, M. Simionescu, Microvascular Research **79**, 154-159 (2010).
5. P. Dalquen, Respiration **66**, 12-13 (1999).
6. M. D. Goldman, Diabetes Care **26**, 1915-1918 (2003).
7. D. A. Kaminsky, Diabetes Care, Mar; **27**, 3, 837-838 (2004).
8. M. Marvisi, G. Marani, M. Brianti, Recenti Prog Med. **87**, 623-627 (1996).
9. M. Takagi, M. J. Absalon, K. G. McLure, M. B. Kastan, Cell **123**, 49–63 (2005).
10. A. J. Link, J. Eng, D. M. Schieltz, E. Carmack, G. J. Mize, D. R. Morris, B. M. Garvik, J. R. Yates, Nat Biotechnol **17**, 676–682 (1999).
11. F. Wan, D. E. Anderson, R. A. Barnitz, A. Snow, N. Bidere, L. Zheng, V. Hegde, L. T. Lam, L. M. Staudt, D. Levens, W. A. Deutsch, M. J. Lenardo, Cell **131**, 927–939 (2007).
12. C. M. Carvalho, A. A. Santos, S. R. Pires, C. S. Rocha, D. I. Saraiva, J. P. Machado, E. C. Mattos, L. G. Fietto, E. P. Fontes. PLoS Pathog **4**, e1000247 (2008).
13. W. Yang, D. Di Vizio, M. Kirchner, H. Steen, M. Freeman, R Mol Cell Proteomics **9**, 54-70 (2010).
14. X. Zhou, W.J. Liao, J.M. Liao, P. Liao, H. Lu, J Mol Cell Biol. **7**, 92-104 (2015).
15. S. Degermann, C. Reilly, B. Scott, L. Ogata, H. von Boehmer, D. Lo, Eur. J. Immunol. **24**, 3155–3160 (1994).
16. N. Simionescu, M. Simionescu, G. E. Palade, J. Cell. Biol. **64**, 586–607 (1975).
17. R. M. Boteanu, E. Uyy, V. I. Suica, F. Antohe, Arch Biochem Biophys. **583**, 55-64 (2015).

18. E. Uyy, L. Ivan, R. M. Boteanu, V. I. Suica, F. Antohe, *Cell Tissue Res* **354**, 771–781 (2013).
19. Y. Zhang, H. Lu, *Cancer Cell* **16**, 369-377 (2009).
20. M. Hong, H. Kim, I. Kim, *Biochem Biophys Res Commun.* **450**:673-678 (2014).
21. J.L. Henry, D.L. Coggin, C.R. King, *Cancer Res.* **53**, 1403-1408 (1993).
22. C. J. Huang, C.C. Chien, S. H. Yang, C. C. Chang, H. L. Sun, Y. C Cheng, C. C. Liu, S. C. Lin, C. M. Lin, *J Cell Mol Med.* **12**, 1936-1943 (2008).
23. Y. A. Hsu, H. J. Lin, J. J. Sheu, F. K. Shieh, S. Y. Chen, C. H. Lai, F. J. Tsai, L. Wan, B. H. Chen, *DNA Cell Biol* **30**, 671-679 (2011).
24. K. Kuroda, M. Takenoyama, T. Baba, Y. Shigematsu, H. Shiota, Y. Ichiki, M. Yasuda, H. Uramoto, T. Hanagiri, K. Yasumoto, *Cancer Sci* **101**, 46-53 (2010).
25. A. Bee, D. Brewer, C. Beesley, A. Dodson, S. Forootan, T. Dickinson, P. Gerard, B. Lane, S. Yao, C. S. Cooper, M. B. Djangoz, C. M. Gosden, Y. Ke, C. S. Foster, *PLoS One* **6**, e22672 (2011).
26. A. Artero-Castro, M. Perez-Alea, A. Feliciano, J. A. Leal, M. Genestar, J. Castellvi, V. Peg, Y. Ramón, S. Cajal, M. E. Leonart, *Autophagy.* **15**, 0 (2015).
27. C. Hu, W. Huang, H. Chen, G. Song, P. Li, Q. Shan, X. Zhang, F. Zhang, H. Zhu, L. Wu, Y. Li, *PLoS One* **10**, e0126643 (2015).
28. N. K. Lee, M. Kim, J. H. Choi, E. B. Kim, H. G. Lee, S. K. Kang, Y. J. Choi, *Peptides* **31**, 2247-2254 (2010).
29. H. Naora, I. Takai, M. Adachi, H. Naora, *J. Cell Biol.* **141**, 741-753 (1998).
30. X. Gao, F. Wan, K. Mateo, E. Callegari, D. Wang, W. Deng, J. Puente, F. Li, M. S. Chaussee, B. B. Finlay, M. J. Lenardo, P. R. Hardwidge, *PLoS Pathog* **5**, e1000708 (2009).
31. F. Wan, A. Weaver, X. Gao, M. Bern, P. R. Hardwidge, M. J. Lenardo, *Nat Immunol.* **12**, 335-343 (2011).
32. X. Gao, P. R. Hardwidge, *Front Microbiol.* **27**, 2,137 (2011).
33. D. Karan, D. L. Kelly, A. Rizzino, M. F. Lin, S. K. Batra, *Carcinogenesis* **23**, 967-975 (2002).
34. Z. Shen, W. Gong, *Ann Transplant* **20**, 312-319 (2015).